Available online at www.sciencedirect.com
SCIENCE DIRECT
Measurement 39 (2006) 553–564
Measurement
www.elsevier.com/locate/measurement

Wavelets and wavelet packets applied to detect and characterize transient alarm signals from termites

Juan José González de la Rosa [a,*], I. Lloret [b], A. Moreno [c], C.G. Puntonet [d], J.M. Górriz [e]

[a] University of Cádiz, Research Group TIC168 – Computational Electronics Instrumentation, Electronics Area, EPSA, Av. Ramón Puyol S/N, E-11202-Algeciras-Cádiz, Spain
[b] University of Cádiz, Research Group TIC168, Spain
[c] Department of Electronics, University of Córdoba, Spain
[d] Department of Architecture and Computers Technology, University of Granada, Spain
[e] Department of Signal Processing, University of Granada, Spain

Received 21 January 2005; accepted 17 November 2005
Available online 10 January 2006

Abstract

In this paper we show the possibility of using wavelets and wavelet packets to detect and characterize alarm signals produced by termites. A set of synthetics have been modelled by mixing the real acquired transients with computer generated noise processes. Identification has been performed by means of analyzing the impulse responses of three sensors undergoing natural excitations. De-noising exhibits good performance up to SNR = −30 dB, in the presence of white gaussian noise. The test can be extended to similar vibratory or acoustic signals resulting from impulse responses.
© 2005 Elsevier Ltd. All rights reserved.

Keywords: Acoustic emission; Seismic accelerometer; Termite characterization; Transient detection; Ultrasonics; Vibratory signal; Wavelets; Wavelet packets

1. Introduction

In acoustic emission (AE) signal processing a customary problem is to extract some physical parameters of interest in situations which involve join variations of time and frequency. This situation can be found in almost every non-destructive AE tests for characterization of defects in materials, or detection of spurious transients which reveals machinery faults [1]. The problem of termite detection lies in this set of applications involving non-stationary signals [2].

When wood fibers are broken by termites they produce acoustic signals which can be monitored using ad hoc resonant acoustic-emission (AE) piezoelectric sensors which include microphones and accelerometers, targeting subterranean infestations by means of spectral and temporal analysis. The drawback is the relative high cost and their practical limitations [2].

* Corresponding author. Tel.: +34 956028020; fax: +34 956028001.
E-mail address: juanjose.delarosa@uca.es (J.J.G. de la Rosa).

0263-2241/$ - see front matter © 2005 Elsevier Ltd. All rights reserved.
doi:10.1016/j.measurement.2005.11.021

In fact, the usefulness of acoustic techniques for detection depends on several biophysical factors. The main one is the amount of distortion and attenuation as the sound travels through the soil ($\sim$600 dB m^{-1}, compared with 0.008 dB m^{-1} in the air). Furthermore, soil and wood are far from being ideal acoustic propagation media because of their high anisotropy and frequency dependent attenuation characteristics [3]. This is the reason whereby signal processing techniques emerged as an alternative.

Second order methods (i.e. correlation and spectra in the time and frequency domains, respectively) failure in low SNR conditions even with ad hoc piezoelectric sensors. Higher order statistics, like the bi-spectrum, have proven to be a useful tool for characterization of termites in relative noisy environments using low-cost sensors [4,5]. The computational cost could be pointed out as the main drawback of the technique. This is the reason whereby diagonal bi-spectrum have to be used.

Numerous wavelet-theory-based techniques have evolved independently in numerous and different signal processing applications, like wavelets series expansions, multiresolution analysis, sub-band coding, image compression, etc. The wavelet transform is a well-suited technique to detect and analyze events occurring to different scales [6]. This suggests the possibility of concentrating on transients and non-stationary movements, making possible the detection of singularities and sharp transitions. And this in turn, points to the idea of decomposing a signal into frequency bands, conveying the possibility of extracting sub-band information which could characterize the physical phenomenon under study [7–9].

In this paper we show an application of wavelets and wavelets packets' de-noising possibilities for the characterization and detection of termite emissions in low SNR conditions. Signals have been buried in gaussian white noise to deteriorate them to the limit. Working with three different sensors we find that the estimated signals' spectra matches the spectra of the acoustic emission whereby the species of termites are biologically identified.

The paper is structured as follows: Section 2 summarizes the problem of acoustic detection of termites; Section 3 remembers the theoretical background of wavelets and wavelet packets, focussing on the analytical tool employed. Section 4 is intended for use as a tool for interpreting results from a wavelet-based experiment. Finally, experiments and conclusions are drawn in Section 5.

2. Acoustic detection of termites

2.1. Characteristics of the AE alarm signals

Acoustic emission (AE) is defined as the class of phenomena whereby transient elastic waves are generated by the rapid (and spontaneous) release of energy from a localized source or sources within a material, or the transient elastic wave(s) so generated (ASTM, F2174-02, E750-04, F914-03[1]). This energy travels through the material as a stress or strain wave and is typically detected using a piezoelectric transducer, which converts the surface displacement (vibrations) to an electrical signal.

Termites use a sophisticated system of vibratory long distance alarm. When disturbed in their nests and in their extended gallery systems, soldiers produce vibratory signals by drumming their heads against the substratum [10]. The drumming signals consist of pulse trains which propagate through the substrate or air (mechanical vibrations), with pulse repetition rates (beats) in the range of 10–25 Hz, with burst rates around 500–1000 ms, depending on the species [10,11]. Soldiers produce such vibratory signals in response to disturbance (1–2 nm by drumming themselves) by drumming their head against the substratum. Workers can perceive these vibrations, become alert and tend to escape. Alarms signals are characterized by high intensity as compared to normal activity signals (movement and feeding), which have low amplitudes. Besides, as said above, alarms have distinctive time patterns.

Fig. 1 shows one of the impulses within a typical four-impulse burst and its associated power spectrum. Significant drumming responses are produced over the range 200 Hz–10 kHz. It is in this interval where the spectral identification of the specie (*Reticulitermes lucifugus*) is performed. The carrier frequency of the drumming signal is defined as the main spectral component, which keeps with longer attenuation time, and in this case is around 2600 Hz.

The spectrum is not flat as a function of frequency as one would expect for a pulse-like event.

[1] American Society for Testing and Materials. F2174-02: Standard Practice for Verifying Acoustic Emission Sensor Response. E750-04: Standard Practice for Characterizing Acoustic Emission Instrumentation. F914-03: Standard Test Method for Acoustic Emission for Insulated and Non-Insulated Aerial Personnel Devices Without Supplemental Load Handling Attachments.

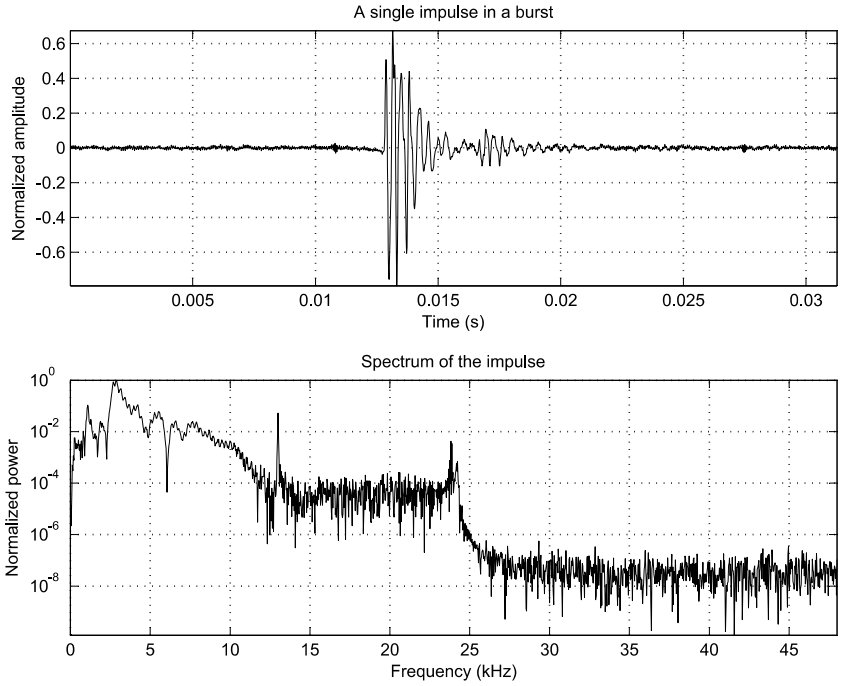

Fig. 1. A single pulse extracted from a four-pulse burst (top) and its associated power spectrum (bottom). Significant amplitudes are found up to 10 kHz. In the interval 10–27 kHz the activity remains constant in a lower energy level.

This is due to the frequency response of the sensor (its selective characteristics) and also to the frequency-dependent attenuation coefficient of the propagation media, wood and air.

2.2. AE types, devices, ranges of measurement and HOS techniques

Two ideal basic types of acoustic emissions are commonly distinguished according to their time instances. Continuous acoustic emission is the most difficult to characterize when several emissions coexist in the same time-series, interfering each other and, consequently making difficult the task of extracting useful information. This is for example the case a sensor output buried in noise. When the measurand is the whole continuous sequence of AE signals, it is best measured as RMS.

Burst-type emission is best characterized by threshold crossing detection. The AE signal voltage is compared with an internally generated reference (threshold). Each time the signal crosses the threshold level, the detecting device emits a pulse (count) which is summed up by a processor. The total count is provided in a time interval (measurement time). When the instrument fails to detect a pulse within a specified timeout, the detector circuit turns off and stores the pulses in the measuring time as a hit.[2]

The former AE types are found in real situations in miscellaneous forms with noise background. Spiky continuous noise characterizes turbulence in fluid or gas flow systems and voltage fluctuations in high tension lines. Characterization helps establish the quality of the energy flow.

Burst-type emission with continuous noise background can be observed in the following situations: cavitation phenomena in fluid flow systems, discharges in power transformers with core noise, signals from leakage in flat-bottom storage tanks and machinery monitoring applications on bearings and gears.

Acoustic measurement devices have been used primarily for detection of termites in wood (feeding and excavating), but there is also the need of detecting termites in trees and soil surrounding building perimeters. Soil and wood have a much longer coefficient of sound attenuation than air, and the coefficient increases with frequency. This attenuation reduces the detection range of acoustic emission to

[2] In the case of the widely used system AED-2000, the timeout period is called *hit determination time* and is 1 ms.

2–5 cm in soil and 2–3 m in wood, as long as the sensor is in the same piece of material [12]. The range of acoustic detection is much greater at frequencies <10 kHz, and low-frequency accelerometers have been used to detect insect larvae over 1–2 m in grain and 10–30 cm in soil [13].

It has been shown that the independent component analysis (ICA) success in separating termite emissions with small energy levels in comparison to the background noise. This is explained away by statistical independence basis of ICA, regardless of the energy associated to each frequency component in the spectra [5]. The same authors have proven that the diagonal bi-spectrum can be used as a tool for characterization purposes [4]. With the aim of reducing computational complexity wavelets transforms have been used in this paper to de-noise corrupted impulse trains.

3. The wavelet transform

3.1. Continuous wavelet transform (CWT)

A *mother wavelet* is a function ψ with finite energy,[3] and zero average

$$\int_{-\infty}^{+\infty} \psi(t)\,\mathrm{d}t = 0. \tag{1}$$

This function is normalized[4], $\|\psi\| = 1$, and is centered in the neighborhood of $t = 0$.

$\psi(t)$ can be expanded with a scale parameter a, and translated by b, resulting the daughter functions or wavelet atoms, which remain normalized

$$\psi_{a,b}(t) = \frac{1}{\sqrt{a}}\psi\left(\frac{t-b}{a}\right). \tag{2}$$

The CWT can be considered as a correlation between the signal under study $s(t)$ and the wavelets (*daughters*). For a real signal $s(t)$, the definition of CWT is

$$\mathrm{CWT}\,s(a,b) = \frac{1}{\sqrt{a}}\int_{-\infty}^{+\infty} s(t)\psi^*\left(\frac{t-b}{a}\right)\mathrm{d}t, \tag{3}$$

where $\psi^*(t)$ is the complex conjugate of the mother wavelet $\psi(t)$, $s(t)$ is the signal under study, and a and b are the scale and the position respectively ($a \in \Re^+ - 0, b \in \Re$). The scale parameter is proportional to the reciprocal of frequency.

[3] $f \in \mathbf{L}^2(\Re)$, the space of the finite energy functions, verifying $\int_{-\infty}^{+\infty} |f(t)|^2\,\mathrm{d}t < +\infty$.

[4] $\|f\| = (\int_{-\infty}^{+\infty} |f(t)|^2\,\mathrm{d}t)^{1/2} = 1$.

The expression for the modulus of CWT is

$$|\mathrm{CWT}\,s(a,b)| = k(a)^{\alpha}, \tag{4}$$

where α is the so-called Lipschitz exponent and k is a constant. Looking at Eq. (4) one can discriminate the signal from the noise by analyzing the local maxima of $|\mathrm{CWTs}(a,b)|$ across the scales.

3.2. Wavelet bases

Any finite energy signal $s(t)$ can be decomposed over a wavelet orthogonal basis [6][5] of $\mathbf{L}^2(\Re)$ according to

$$s(t) = \sum_{j=-\infty}^{+\infty}\sum_{k=-\infty}^{+\infty} \langle s, \psi_{j,k}\rangle\psi_{j,k}. \tag{5}$$

Each partial sum, indexed by k, in Eq. (5) can be interpreted as the details variations at the scale $a = 2^j$

$$d_j(t) = \sum_{k=-\infty}^{+\infty} \langle s, \psi_{j,k}\rangle\psi_{j,k} \qquad s(t) = \sum_{j=-\infty}^{+\infty} d_j(t). \tag{6}$$

The approximation of the signal $s(t)$ can be progressively improved by obtaining more layers or levels, with the aim of recovering the signal selectively. For example, if $s(t)$ varies smoothly we can obtain an acceptable approximation by means of removing fine scale details, which contain information regarding higher frequencies or rapid variations of the signal. This is done by truncating the sum in (9) at the scale $a = 2^J$

$$s_J(t) = \sum_{j=J}^{+\infty} d_j(t). \tag{7}$$

3.3. Discrete time wavelet transform (DTWT)

In the DTWT the original signal passes through two complementary filters and two signals are obtained as a result of a downsampling process, corresponding to the approximation and detail coefficients. The lengths of the detail and approximation coefficient vectors are slightly more than half the length of the original signal, $s(t)$. This is the result of the digital filtering process (convolution) [7]. The approximations are the high-scale, low-frequency components of the signal. The details are the low-scale, high-frequency components.

A tree-structure arrangement of filters allows the sub-band decomposition of the signal. In each stage

[5] $\{\psi_{j,k}(t) = \frac{1}{\sqrt{2^j}}\psi(\frac{t-2^j k}{2^j})\}_{(j,k)\in\mathbb{Z}^2}$.

of the filtering process the same two digital filters are used: a high pass $h_a(\cdot)$, the discrete mother, and its mirror filter (low pass) $g_a(\cdot)$. All these filters have the same relative bandwidth (ratio between frequency bandwidth and center frequency). The results of the decomposition can be expressed as

$$\mathrm{DTWT}\, s(j,n) = \sum_{k=0}^{N-1} h_j(2^{j+1}n - k)s(k), \tag{8}$$

where N is the number of samples in the signal, j is the decomposition level, n is the time shifting. The same arguments are valid for the process of reconstruction.

3.4. Wavelet packets (WP)

3.4.1. A brief presentation

The WP method is a generalization of wavelet decomposition that offers more possibilities of reconstructing the signal from the decomposition tree. If L is the number of levels in the tree, WP methods yields more than $2^{2^{L-1}}$ ways to encode the signal. The wavelet decomposition tree is a part of the complete binary tree.

When performing a split we have to look at each node of the decomposition tree and quantify the information to be gained as a result of a split. An entropy based criterion is used herein to select the optimal decomposition of a given signal. We use an adaptative filtering algorithm, based on the work by Coifman and Wickerhauser [14].

We start from the functions w_n and we built a family of analyzing functions

$$\left\{ w_{n,j,k}(t) = \frac{1}{\sqrt{2^j}} w_n\left(\frac{t - 2^j k}{2^j}\right) \right\}_{(j,k)\in\mathbb{Z}^2}, \tag{9}$$

where $n \in \mathbb{N}$ is the frequency, k is the time-localization parameter and j is the scale. The idea of wavelet packets is that for fixed values of k and j, $w_{n,j,k}$ analyzes the fluctuations of the signal under study around the position $2^j k$, for the scale 2^j, and for various frequencies depending on the admissible values of n. For each scale 2^j, the possible values of the parameter n are $0, 1, \ldots, 2^j - 1$. The set of functions $w_{j,n}$ is the wavelet packet. Some theoretical background is introduced to understand multiresolution analysis.

3.4.2. Bases' splitting: Multiresolution

We consider the resolution as the time step 2^{-j}, for a scale j, as the inverse of the scale 2^j. The approximation of a function $s(t)$ at a resolution 2^{-j} is defined as an orthogonal projection over a space $\mathbf{V}_j \subset \mathbf{L}^2(\Re)$. $\mathbf{V}_j$ is called the scaling space and contains all possible approximations at the resolution 2^{-j}. The orthogonal projection of s, $P_{\mathbf{V}_j}s$, over the space, is a function $s_j \subset \mathbf{V}_j$ that minimizes the difference given by the approximation error, $\|s - s_j\|$. For a zero resolution we loose all the details of s, and when the resolution goes to ∞, $s_j = s$

$$\lim_{j\to+\infty} \|s_j\| = 0, \qquad \lim_{j\to-\infty} \|s - s_j\| = 0. \tag{10}$$

As a consequence, as the resolution increases, the error tends to 0. This tendency depends on the regularity of the signal $s(t)$ [6].

Let us consider a scaling function ϕ. Dilating and translating this function we obtain an orthonormal basis of $\mathbf{V}_j$

$$\left\{ \phi_{j,k}(t) = \frac{1}{\sqrt{2^j}} \phi\left(\frac{t - 2^j k}{2^j}\right) \right\}_{(j,k)\in\mathbb{Z}^2}. \tag{11}$$

The approximation of a signal s at a resolution 2^{-j} is the orthogonal projection over the scaling subspace $\mathbf{V}_j$, and is obtained with an expansion in the scaling orthogonal basis $\{\phi_{j,k}\}_{k\in\mathbb{Z}}$

$$P_{\mathbf{V}_j}s = \sum_{k=-\infty}^{+\infty} \langle s, \phi_{j,k}\rangle \phi_{j,k}. \tag{12}$$

The inner products

$$a_j[k] = \langle s, \phi_{j,k}\rangle \phi_{j,k} \tag{13}$$

represent a discrete approximation of the signal al level j (scale 2^j). This approximation represents the low-pass filtering of s, sampled at intervals 2^{-j}.

A fast wavelet transform decomposes successively each approximation $P_{\mathbf{V}_j}s$ into a coarser approximation $P_{\mathbf{V}_{j+1}}s$ (local averages, approximation) plus the wavelet coefficients carried by $P_{\mathbf{W}_{j+1}}s$ (local details). The smooth signal plus the details combine into a multiresolution of the signal at the finer level $j+1$. Averages come from the scaling functions and details come from the wavelets.

$\{\phi_{j,k}\}_{k\in\mathbb{Z}}$ and $\{\psi_{j,k}\}_{k\in\mathbb{Z}}$ are orthonormal bases of $\mathbf{V}_j$ and $\mathbf{W}_j$, respectively, and the projections on these spaces are characterized by

$$a_j[k] = \langle s, \phi_{j,k}\rangle, \qquad d_j[k] = \langle s, \psi_{j,k}\rangle. \tag{14}$$

So, if $\psi(t)$ and $\phi(t)$ are the wavelet and the scale functions, respectively, the wavelet decomposition of a given signal $s(t)$ at a given level J can be expressed by

$$s(t) = \sum_{k=-\infty}^{+\infty} a_J[k]\phi_{J,k}(t) + \sum_{j=1}^{J}\sum_{k=-\infty}^{+\infty} d_j[k]\psi_{j,k}(t), \tag{15}$$

where $\{a_J[k], k \in \mathbf{Z}\}$ represents the coarser resolution signal at the level J, and $\{d_j[k],\ j = 1,\ldots,J;\ k \in \mathbf{Z}\}$, are the wavelet coefficients containing the information about the highest frequencies of the signal.

Thus, the multiresolution decomposition is in essence a frequency analysis of the signal with good temporal information. The signal is decomposed in frequency bands (sub-bands), making a dyadic decomposition of the frequency range. Hence, in each resolution level a new signal is built which contains a frequency band of the original signal which characterizes its local features. Thus, for level j, wavelet coefficients are distributed along 2^j points.

The former lines convey the idea of decomposition of a vectorial space in the direct sum of two new subspaces. A space $\mathbf{V}_{j-1}$ is decomposed in a lower resolution space $\mathbf{V}_j$ plus a detail space $\mathbf{W}_j$, dividing the orthogonal basis of $\mathbf{V}_{j-1}$ into two new orthogonal bases

$$\{\phi_j(t-2^j k)\}_{k\in\mathbb{Z}}, \qquad \{\psi_j(t-2^j k)\}_{k\in\mathbb{Z}}. \tag{16}$$

$\mathbf{W}_j$ is the orthogonal complement of $\mathbf{V}_j$ in $\mathbf{V}_{j-1}$, and $\mathbf{V}_j \subset \mathbf{V}_{j-1}$, thus

$$\mathbf{V}_{j-1} = \mathbf{V}_j \oplus \mathbf{W}_j. \tag{17}$$

The orthogonal projection of a signal $s(t)$ on $\mathbf{V}_{j-1}$ is decomposed as the sum of orthogonal projections on $\mathbf{V}_j$ and $\mathbf{W}_j$.

$$P_{\mathbf{V}_{j-1}} = P_{\mathbf{V}_j} + P_{\mathbf{W}_j}. \tag{18}$$

The recursive splitting of these vector spaces is represented in the binary tree. This fast wavelet transform is computed with a cascade of filters $\bar{h}$ and $\bar{g}$, followed by a factor 2 subsampling, according with the scheme of Fig. 2.

For example, if we consider a signal defined in the time interval $0 \leqslant t < 1$, and sampled at 1/256, the original data are considered to be the coefficients in the expansion of the original continuous signal in terms of the basis functions $\phi_{j,k}$ with $j = 8$ and $k = 0,\ldots,255$. In wavelet packets transforms these data are decomposed in two blocks of data, each half size of the original data, by convolving with filters h and g, respectively. Further decomposition will split each 128-sized block into two 64-sized blocks, and so on. In each level the block obtained from convolving with the low-pass filter h is on the left.

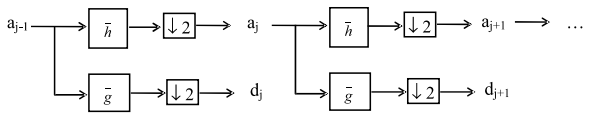

Fig. 2. Cascade of filters and subsampling.

In order to choose the most appropriate decomposition of the signal a contrast function is required. Functions that verify additivity-type property are suitable for efficient searching of the tree structures and node splitting. The criteria based on the entropy match these conditions, providing a degree of randomness in an information-theory frame. In this work we used the entropy criteria based on the p-norm

$$E(s) = \sum_i^N \|s_i\|^p \tag{19}$$

with $p \leqslant 1$, and where $s = [s_1, s_2, \ldots, s_N]$ in the signal of length N.

The results are accompanied by entropy calculations based on Shannon's criterion

$$E(s) = -\sum_i^N s_i^2 \log(s_i^2) \tag{20}$$

with the convention $0 \times \log(0) = 0$.

3.5. Estimation of signals in additive noise

The estimation of signal s is performed by an operator that attenuates the noise and preserves the signal. In wavelets and wavelet packets thresholding estimators are used to suppress additive noise and recover signal which have been degraded by low-pass filtering [6].

Considering the N-point noisy signal, x, as a mixture of the signal, s, plus the additive noise, n (of variance σ^2), $x = s + n$, a diagonal estimator of s from x can be expressed as

$$\hat{s} = Dx = \sum_{m=0}^{N-1} d_m(x_B[m]) g_m, \tag{21}$$

where D is a diagonal operator in an orthonormal basis $B = \{g_m\}_{0\leqslant m\leqslant N}$; and d_m are thresholding functions [6,15].

Choosing the threshold $T = \sigma\sqrt{2\ln N}$, the estimator of the signal, $\hat{s}$, is at least as regular as s, because the wavelets coefficients have a smaller amplitude. This is true for soft thresholding estimators. Hard estimators leave unchanged the coefficients above the threshold T, and consequently their coefficients can be larger due to the presence of noise.

Some traces of the noise remain nearby the singularities if hard thresholding is chosen. The removing action takes place where the signal s is regular. The soft thresholding estimation reduces the noise effect in the discontinuities at the price of reducing by T the amplitude of the coefficients. As a rule of thumb, once hard thresholding is performed, the parameter T for soft thresholding is obtained reducing by two the optimal hard threshold.

4. Pre-experimental practical examples

Before analyzing the specific experience of termite emissions, some practical examples help understand how to design wavelets-based experiences and how to interpret the concepts of scale and multiresolution. Scale is easily understood using the simplest mother, the *Haar* wavelet. Haar wavelet is discontinuous, resembles a step function, and represents the same wavelet as Daubechies db1. Fig. 3 represents de CWT of 5 cycles of a sinusoidal wave with a resolution of 1000 points/cycle. The Haar wavelet supports is up to 1 unit of time. This time support can bee seen in the middle graph. If we consider scale 1000 we have to consider that for every 1000 points of our signal we have to match them with an unity of time in the wavelet. Fig. 3 is very simple to interpret because the same number of points describe the period of the sine wave and the period of the wavelet. CWT results are absolute values so we have to obtain 10 complete vertical stripes corresponding to the 5 periods of the sinusoidal wave.

The CWT of the hyperbolic chirp in Fig. 4 shows that as the scale increases (lower frequencies) the cone of maxima values opens to the top. The vertex of the cone is located in the center of the diagram, corresponding to the highest instantaneous frequency. Fig. 5 shows the WP analysis of a linear chirp and the WP coefficients from the decomposition tree. Among these coefficients there are many choices to form an orthogonal decomposition of our signals. For example, we can choose the coefficients that are all in the same level.

Irregular structures in a signal often convey the idea of hidden essential information in the characterization process. For example, discontinuities in the intensity of an image are associate to edges. Interesting information can be also extracted from sharp transitions in radar and electrocardiograms [6]. These singularities can be detected following

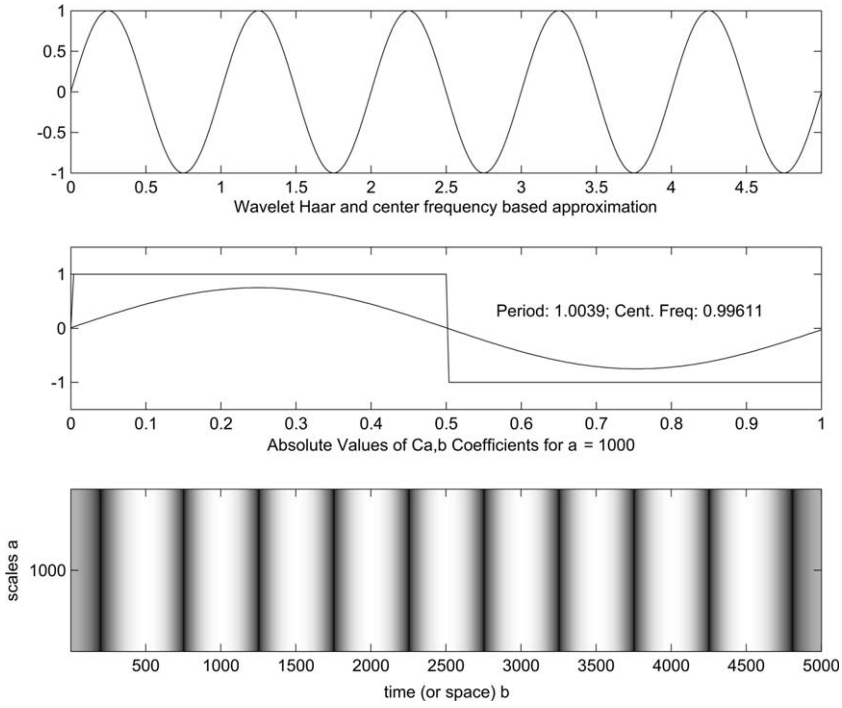

Fig. 3. From top to bottom: 5 cycles of a sinusoidal wave with a resolution of 1000 points per cycle, the wavelet Haar and its center-frequency based approximation (up to 1 unit of time), the CWT diagram corresponding to scale 1000 (white zones correspond to maxima area).

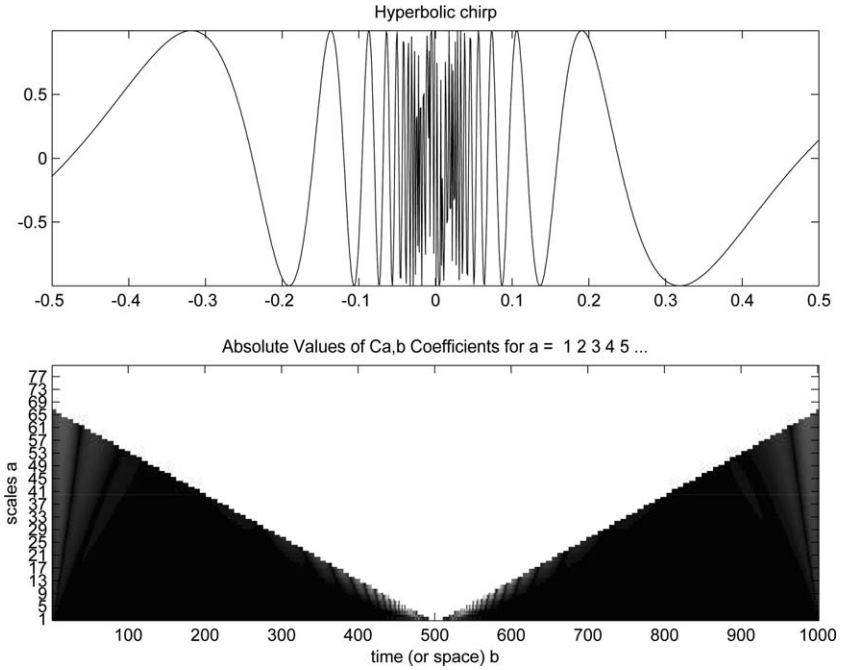

Fig. 4. Simulation of a hyperbolic chirp and its cone of maxima values. Time extends from -0.5 to 0.5 with a resolution of 0.001 units, which could be seconds. The signal is modelled by $f(t) = \sin(1.5 \times t^{-1})$.

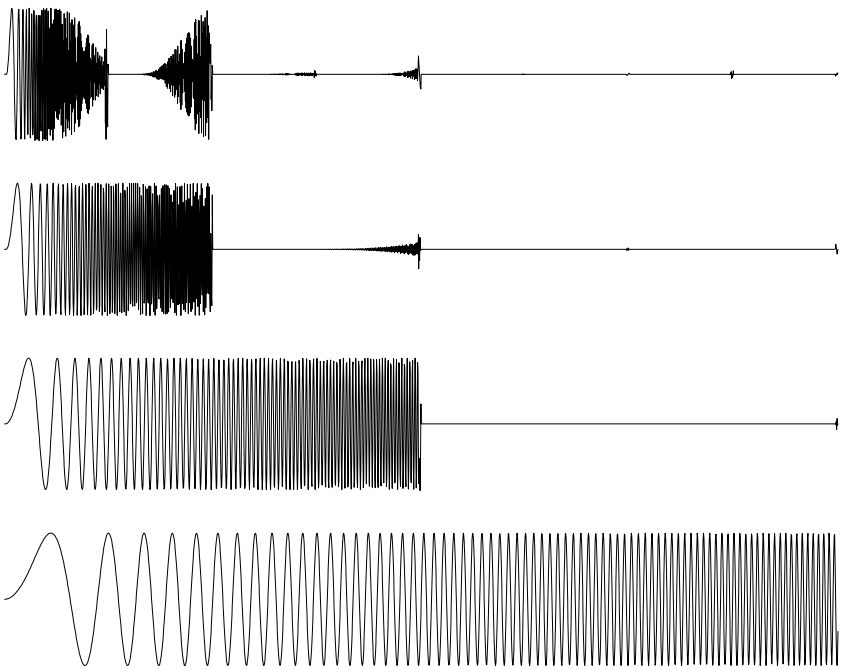

Fig. 5. Simulation of a linear chirp and its wavelet packet analysis up to level 3 using *sym*8. From bottom to top and from left to right the depth position is: $(0,0)$, $(1,0)$, $(1,1)$, $(2,0),\ldots,(2,3)$, $(3,0),\ldots,(3,7)$.

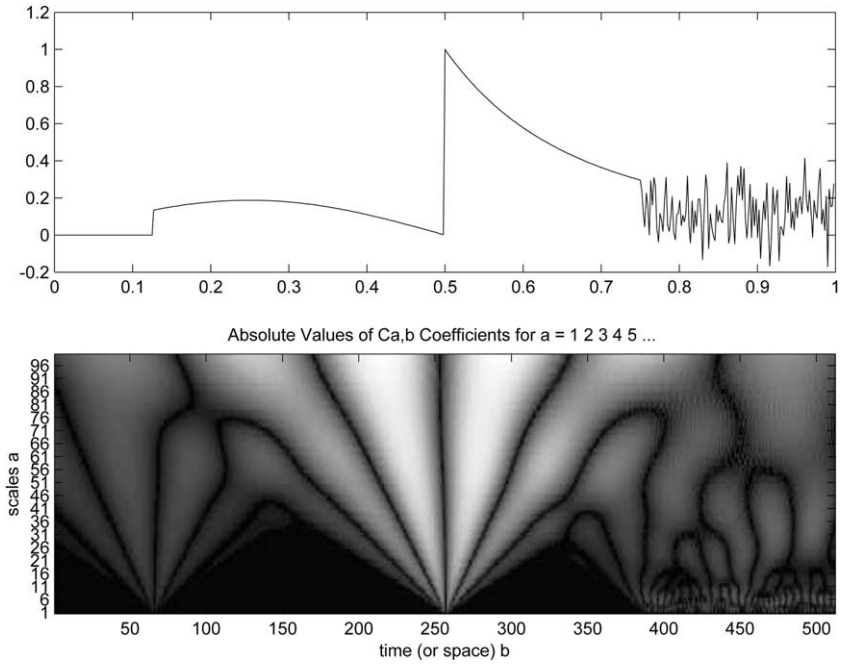

Fig. 6. A prototype signal (top) exhibiting singularities, which originate large values of amplitude coefficients in their cones of influence (bottom graph). The wavelet Gaussian Derivative Wavelet *gaus*8 has been employed.

the maxima of the CWT. The prototype hand-made function (inspired by [6]) of Fig. 6 includes several singularities. This last example, in Fig. 6, shows that wavelet coefficients provide explicit information on the location and type of signal singularities.

The rest of the paper presents queue results obtained by means of the tools and examples described here.

5. Experiments and conclusions

Two accelerometers (KB12V, seismic accelerometer; KD42V, industrial accelerometer, MMF) and a standard microphone (Ariston CME6) have been used to collect data (alarm signals from termites) in different places (basements, subterranean wood structures and roots) using the sound card of a portable computer and a sampling frequency of 96,000 (Hz). Table 1 summarizes the main features of the vibration transducers employed. These sensors have different sensibilities and impulse responses. This is the reason whereby we normalize spectra.

The de-noising procedure was developed using a *sym*8, belonging to the family *Symlets* (order 8), which are compactly supported wavelets with least asymmetry and highest number of vanishing moments for a given support width. We also choose a soft heuristic thresholding.

The numerical value of the signal-to-noise ratio is obtained by

$$\mathrm{SNR}_{\mathrm{dB}} = 10\log_{10}\left(\frac{E\{\|s\|^2\}}{E\{\|n\|^2\}}\right), \tag{22}$$

where $s(t)$ an $n(t)$ and the signal of interest before corrupting and the noise, respectively. In Eq. (22), signals have been considered zero mean.

We used 20 registers (from *Reticulitermes grassei*), each of them comprises a four-impulse burst buried in white gaussian noise. De-noising performs successfully up to an SNR $= -30$ dB. Fig. 7 shows a

Table 1
Main characteristics of the transducers

Transducer	Type	Sensitivity	Bandwidth
KD42V (MMF)	Piezo-accelerometer	10.03 mV/m/s^2	100 Hz–100 kHz
KB12V (MMF)	Piezo-accelerometer	517.1 mV/m/s^2	100 Hz–100 Hz
CME6 (Ariston)	Directional micro.	62 ± 3 dB	100 Hz–8 kHz

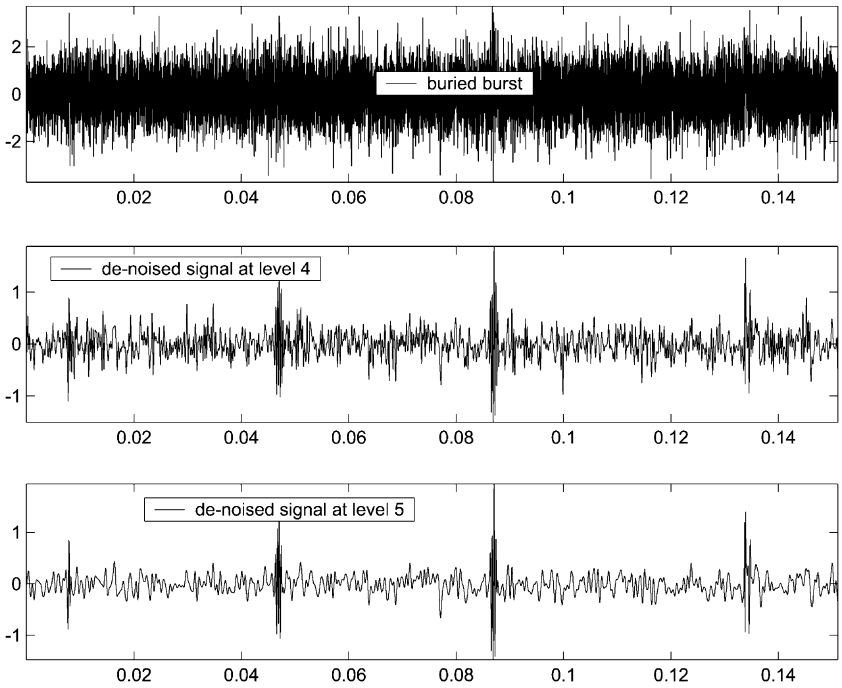

Fig. 7. Limit situation of the de-noising procedure using wavelets (SNR = −30 dB). From top to bottom: a buried four-impulse burst, estimated signal at level 4, estimated signal at level 5. Time resolution: 1/96,000 (s).

de-noising result in one of the registers. Fig. 8 shows a comparison between the spectrum of the estimated signal at level 4 and the spectrum of the signal to be de-noised, taking a register as an example. Signifi-

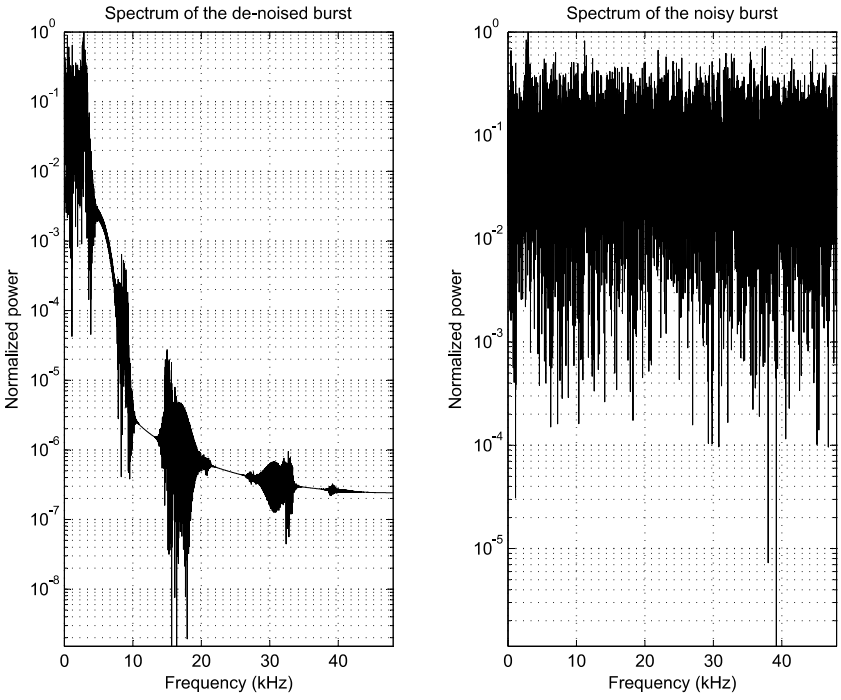

Fig. 8. Spectra of the estimated signal (left) and the buried burst.

cant components in the spectrum of the recovered signal are found to be proper of termite emissions.

The same 20 registers were processed using wavelet packets. Approximation coefficients have been

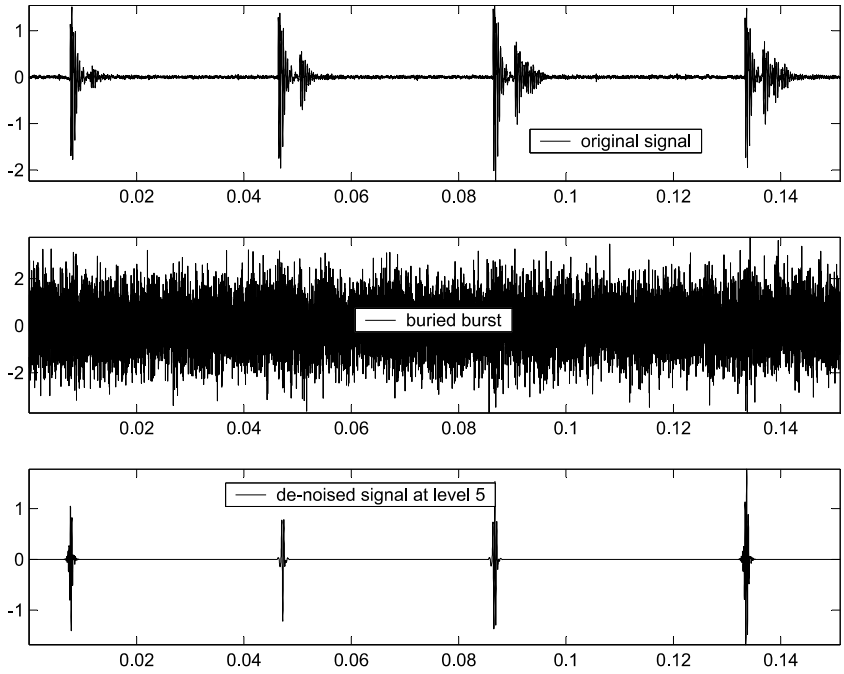

Fig. 9. Limit situation of the de-noising procedure using WP (SNR = −30 dB). From top to bottom: original signal, a buried four-impulse burst, estimated signal at level 5. Time resolution: 1/96,000 (s).

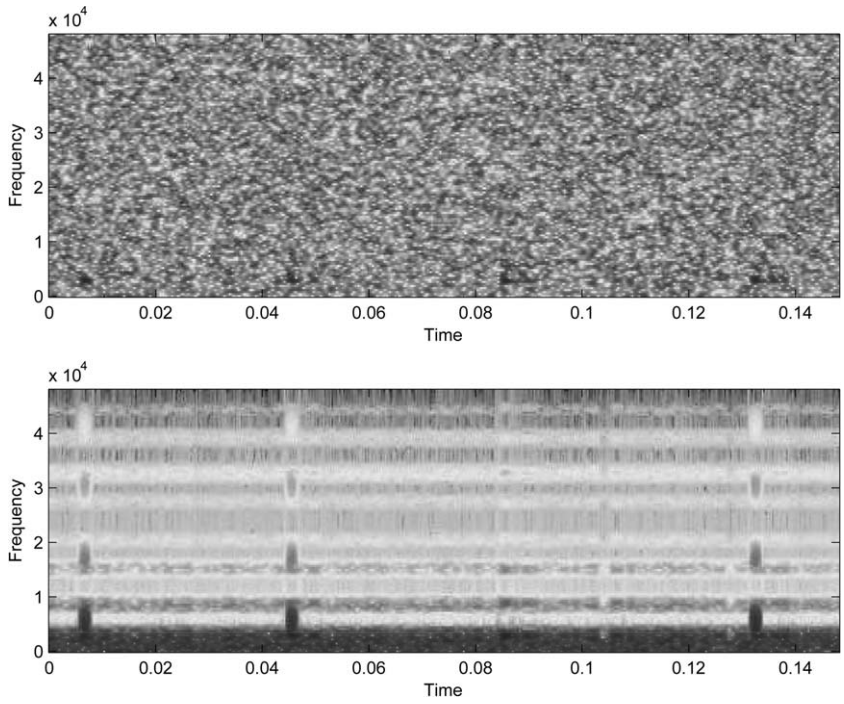

Fig. 10. Example of spectrogram comparison: corrupted four-impulse burst (above) vs. cleaned signal.

truncated by thresholding in order to obtain a more precise estimation of the starting points for each impulse. Stein's Unbiased Estimate of Risk (SURE) has been assumed as a principle for selecting a threshold to be used for de-noising. A more thorough discussion of choosing the optimal decomposition can be found in [6]. Fig. 9 shows one of the 20 de-noised signals using wavelets packets. It can be seen that the result of reconstructing progressively each a_j by the filter banks improves the estimation of the time of occurrence of the impulses and the burst.

In order to use a speech-enhancement comparison tool we have performed a spectrogram comparison [16] between a corrupted burst and the cleaned output (SR = −30 dB). One of the comparisons is depicted in Fig. 10, which represents the most probable result in the spectrogram comparison stage. We can see 3 temporal regions with high coefficients. The region corresponding to the third impulse could not be enhanced. In other registers' comparisons the most probable situation is the lack of one impulse in the four-impulse burst. We adopted the criteria of identifying the de-noise process as success if at least three impulses are detected.

On the other hand, it can be observed that the contents of noise are decreased in the enhanced version. Although the noise remains high in a strong-energy region, it is masked by the de-noised signal.

Acknowledgements

The authors would like to thank the Spanish Ministry of Science and Education for funding the projects DPI2003-00878, and PTR95-0824-OP. The first one deals with noise modelling and measurement. The second one is oriented to develop termite detection algorithms.

References

[1] X. Lou, K.A. Loparo, Bearing fault diagnosis based on wavelet transform and fuzzy inference, Mechanical Systems and Signal Processing 18 (5) (2004) 1077–1095.

[2] J.J.G. de la Rosa, C.G. Puntonet, J.M. Górriz, I. Lloret, An application of ica to identify vibratory low-level signals generated by termites, in: Proceedings of the Fifth International Conference, ICA 2004, Granada, Spain. Lecture Notes in Computer Science (LNCS), vol. 3195, 2004, pp. 1126–1133.

[3] R.W. Mankin, J.R. Fisher, Current and potential uses of acoustic systems for detection of soil insects infestations, in: Proceedings of the Fourth Symposium on Agroacoustic, 2002, pp. 152–158.

[4] J.J.G. de la Rosa, I. Lloret, C.G. Puntonet, J.M. Górriz, Higher-order statistics to detect and characterise termite emissions, Electronics Letters 40 (20) (2004) 1316–1317, ultrasosics.

[5] J.J.G. de la Rosa, C.G. Puntonet, I. Lloret, An application of the independent component analysis to monitor acoustic emission signals generated by termite activity in wood, Measurement 37 (1) (2005) 63–76, available online 12 October 2004.

[6] S. Mallat, A Wavelet Tour of Signal Processing, second ed., Academic Press, 1999.

[7] L. Angrisani, P. Daponte, M. D'Apuzzo, A method for the automatic detection and measurement of transients, part I: The measurement method, Measurement 25 (1) (1999) 19–30.

[8] L. Angrisani, P. Daponte, M. D'Apuzzo, A method for the automatic detection and measurement of transients, part II: Applications, Measurement 25 (1) (1999) 31–40.

[9] M. Boltezăr, J. Slavič, Enhancements to the continuous wavelet transform for damping identifications on short signals, Mechanical Systems and Signal Processing 18 (1) (2004) 1065–1076.

[10] A. Röhrig, W.H. Kirchner, R.H. Leuthold, Vibrational alarm communication in the African fungus-growing termite genus macrotermes (isoptera, termitidae), Insectes Sociaux 46 (1999) 71–77.

[11] S. Connétable, A. Robert, F. Bouffault, C. Bordereau, Vibratory alarm signals in two sympatric higher termite species: *Pseudacantotermes spiniger* and *P. militaris* (termitidae, macrotermitinae), Journal of Insect Behaviour 12 (3) (1999) 90–101.

[12] R.W. Mankin, W.L. Osbrink, F.M. Oi, J.B. Anderson, Acoustic detection of termite infestations in urban trees, Journal of Economic Entomology 95 (5) (2002) 981–988.

[13] W.P. Robbins, R.K. Mueller, T. Schaal, T. Ebeling, Characteristics of acoustic emission signals generated by termite activity in wood, in: Proceedings of the IEEE Ultrasonic Symposium, 1991, pp. 1047–1051.

[14] R.R. Coifman, M. Wickerhauser, Entropy-based algorithms for best basis selection, IEEE Transactions on Information Theory 38 (2) (1992) 713–718.

[15] G. Strang, T. Nguyen, Wavelets and Filter Banks, first ed., Wellesley-Cambridge Press, 1997.

[16] C.-T. Lu, H.-C. Wang, Speech enhancement using perceptually constrained gain factors in critical-band-wavelet-packet transform, Electronics Letters 40 (6) (2004) 394–396, speech Processing.